H2O2 Enhances the Anticancer Activity of TMPyP4 by ROS-mediated Mitochondrial Dysfunction and DNA Damage

Jianqiang Chen
Wenzhou Medical College - Chashan Campus: Wenzhou Medical University
Xiangxiang Jin
Wenzhou Medical College - Chashan Campus: Wenzhou Medical University
Zhe Shen
Wenzhou Medical College - Chashan Campus: Wenzhou Medical University
Yanan Mei
Wenzhou Medical College - Chashan Campus: Wenzhou Medical University
Jufang Zhu
Wenzhou Medical College - Chashan Campus: Wenzhou Medical University
Xiaodan Zhang
The Seventh Peoples Hospital of Wenzhou
Guang Liang
Wenzhou Medical College - Chashan Campus: Wenzhou Medical University
Xiaohui Zheng (zhengxh@wmu.edu.cn)
Wenzhou Medical University https://orcid.org/0000-0002-1307-1209

Research Article

Keywords: TMPyP4, ROS, Apoptosis, DNA damage, Tumor microenvironment

Posted Date: February 16th, 2021

DOI: https://doi.org/10.21203/rs.3.rs-189358/v1

Version of Record: A version of this preprint was published at Medical Oncology on April 21st, 2021. See the published version at https://doi.org/10.1007/s12032-021-01505-x.

Abstract

Cancer is one of the diseases that threatens human health and is a leading cause of mortality worldwide. High levels of reactive oxygen species (ROS) have been observed in cancer tissues compared with normal tissues *in vivo*, and it is not yet known how this influences chemotherapeutic drug action. Cationic porphyrin 5,10,15,20-tetra-(N-methyl-4-pyridyl) porphyrin (TMPyP4) is a photosensitizer used in photodynamic therapy (PDT) and a telomerase inhibitor used in the treatment of telomerase-positive cancer. Here, we investigated the anticancer activity of TMPyP4 in A549 and PANC cells cultured in H_2O_2. The results showed that compared to TMPyP4 alone, the combination of TMPyP4 and H_2O_2 exhibited sensitization effects on cell viability and colony formation inhibition and apoptosis in A549 and PANC cells but had no effect in human normal MIHA cells. Mechanistically, the combination of TMPyP4 and H_2O_2 activates high ROS and mitochondrial membrane potential in A549 and PANC cells, resulting in intense DNA damage and DNA damage responses. Consequently, compared to TMPyP4 alone, TMPyP4 and H_2O_2 combined treatment upregulates the expression of BAX, cleaved caspase 3, and p-JNK, and downregulates the expression of Bcl-2 in A549 and PANC cells. Taken together, these data suggested that H_2O_2 enhanced the anticancer activity of TMPyP4-mediated ROS-dependent DNA damage and related apoptotic protein regulation, revealing that the high ROS tumor microenvironment plays an important role in chemotherapeutic drug action.

Introduction

The microenvironment of tumors (TME) is characterized by a high content of reactive oxygen species (ROS), which is a collective term referring to unstable, reactive, partially reduced oxygen derivatives, such as hydrogen peroxide (H_2O_2), superoxide anion (O_2^-), singlet oxygen ($^1O_2$) and hydroxyl radical (·OH) [1, 2]. The elevated ROS in the TME is mainly due to the dismutation of superoxide dismutase in mitochondria [3, 4]. Additionally, the production of ROS is also attributed to the rapid proliferation of tumor cells [5]. It is well established that ROS play a significant role in tumorigenesis and affect numerous biological processes, such as inflammation, genomic instability, metabolic reprogramming, resistance to apoptosis and cell proliferation [6]. Moreover, ROS have been found to be deeply involved in drug resistance [7–9] and the efficacy of antitumor drugs [10]. As described above, ROS are of indisputable importance in cancer development and chemotherapy efficacy. Thus, high ROS in the TME can not only be exploited as a strategy for selective antitumor therapy but also be a priority consideration in antitumor drugs selectivity.

Photodynamic therapy (PDT) induces cancer cell death mainly by ROS, which are produced by irradiated photosensitizers [11]. Since PDT mainly relies on a specific biodistribution of a photosensitizer drug to tumor cells, the choice of photosensitizer is crucial for PDT treatment [12]. However, it has been challenging to obtain an optimal photosensitizer with a high yield of ROS and high precision targeting to cancer cells [12]. Among the available photosensitizer drugs, porphyrins are the most frequently reported in the literature [13, 14]. Of all porphyrin derivatives, TMPyP4 has been considered a promising

photosensitizer due to its high water solubility, limited dark toxicity, high ROS production rate, high permeability through the cell membrane and preferential accumulation in tumor cells [15–17]. In recent years, TMPyP4 has been discovered to also be a G-quadruplex stabilizer that consequently inhibits telomerase activity in telomerase-positive cancer cells [18–20]. Because of this, TMPyP4 might be endowed with greater clinical application prospects than other antitumor drugs because it possesses both photosensitizer and telomerase inhibition activity.

As mentioned above, although the influence of high ROS in the TME on antitumor drug efficiency is not negligible and there is great potential for the clinical application of TMPyP4, the effects of high ROS in the TME on TMPyP4 remain unclear. In this study, we aimed to investigate the antitumor activity of TMPyP4 under TME-related high ROS and to explore the underlying mechanism in both A549 cells and PANC cells.

Materials And Methods

Cell cultures

The non-small cell lung cancer (NSCLC) cell line A549, pancreatic cancer cell line PANC and human normal hepatocyte line MIHA were obtained from the Cell Resource Center of Peking Union Medical College. Cells were cultured in DMEM (Gibco, USA) at 37 °C under 5% CO_2 supplemented with 10% fetal calf serum (Gibco, USA) and 100 U/mL penicillin and streptomycin (HyClone, USA).

Reagents and antibodies

TMPyP4, 5,10,15,20-tetrakis(1-methylpyridinium-4-yl) porphyrin tetra(p-toluenesulfonate) and H_2O_2 were purchased from Sigma and dissolved in water. Antibodies against BAX, Bcl2, caspase 3, cleaved caspase 3, JNK, p-JNK, γ-H2AX, β-actin and HRP-conjugated secondary antibodies were purchased from Cell Signaling Technology (USA). 53BP1 was from EMD Millipore (USA). β-actin was purchased from Proteintech (USA).

Cell viability assay

A549, PANC and MIHA cells were seeded on 96-well plates (3×10^3/well) and then treated with or without 10 μM TMPyP4 for 70 h, later treating them with 800 μM H_2O_2 for 2 h, after which 20 μl of 3-(4,5-dimethylthiazol-2-yl)-2,5-diphenyltetrazolium bromide (MTT) (0.5 mg/ml) was added to each well for another 4h. The formazan reaction product was dissolved in DMSO (100 μl) after discarding the culture medium. Cell viability was detected by reading the absorbance at 490 nm with a Multiskan FC automatic microplate reader (Thermo Fisher, USA).

Measurement of intracellular ROS production

ROS were monitored using a ROS kit (Sigma, USA) according to the manufacturer's instructions. In short, 1.5×10^5 cells were grown in six-well cell culture plates and incubated overnight. After treatment with or without drugs, cells were incubated with 10 μM DCFH-DA for 30 min at 37 °C in the dark. DCF fluorescence intensity was measured by flow cytometry (BD FACS Calibur, BD Biosciences, USA) and Nikon fluorescence microscopy (Nikon, Japan).

Colony formation

A549 and PANC cells were plated into 12-well plates (1000 cells/well) and incubated overnight until the cells attached to the dish and then were exposed to drugs or not. When sufficiently large colonies formed, the cells were washed, fixed with 4% paraformaldehyde and stained with crystal violet. Colonies in each plate were photographed under a light microscope and then the crystals were dissolved in 500 μL acetic acid (33%) and their absorbance was detected at 560 nm by a spectrophotometer.

Apoptosis assay

A549 and PANC cells were seeded in 6 cm^2 dishes (1.5×10^5/well), incubated for 6h until the cells attached to the dish, and then treated with the indicated concentration of drugs. Cells were harvested for the Annexin V/PI apoptosis assay according to the manufacturer's instructions and were analyzed by a flow cytometer.

Measurement of mitochondrial membrane potential (Δψm)

The cell mitochondrial membrane potential was detected by flow cytometry utilizing JC-1 (5,5',6,6'-tetrachloro-1,1',3,3'-tetraethylbenzimi-dazolylcarbocyanine iodide) staining. Briefly, A549 and PANC cells were treated with the indicated drug for the indicated times, harvested, and loaded with JC-1 solution for 20 min at 37 °C in the dark. Red fluorescence and green fluorescence intensity were determined by flow cytometry.

Immunofluorescence (IF) assays

Immunofluorescence (IF) assays were performed as previously described [21]. Cells were fixed with 4% paraformaldehyde, permeabilized with 0.5% Triton X-100 for 30 min, blocked with 5% GS for 1h at 37 °C, and incubated with primary antibodies (53BP1 or cleaved caspase 3) overnight at 4 °C in a humidified chamber. The next day, the cells were incubated with secondary antibody (anti-rabbit 488) for 1.5h at room temperature and mounted with DAPI. Fluorescent images were captured with a Nikon fluorescence microscope.

Comet assays

DNA damage was measured by neutral or alkaline comet assay [22]. In short, cells were treated with or without drugs, collected, and mixed with 0.5% low-melting-temperature agarose before being transferred onto slides, which were coated with 1.5% normal agarose. Then, the slides were lysed in 10 mM Tris (pH 8.0), 3% DMSO, 2.5 M NaCl, 0.5% Triton X-100, 1% N-lauroylsarcosine, and 100 mM EDTA and electrophoresed in 1% DMSO, 100 mM Tris-HCl, 300 mM sodium acetate at 1.5 V/cm for 25 min, mounted with 0.02 mg/mL PI solution and visualized under a Nikon fluorescence microscope. The analysis was performed with CASP.

Western blot analysis

The total protein was extracted and boiled for 10 min. The concentration of protein was detected by a Bradford assay, and the proteins were separated *via* SDS-PAGE and transferred to 0.25 μm PVDF membranes. The membranes were blocked with 5% skim milk (BD, USA) for 2 h at room temperature, incubated with primary antibodies at 4 °C overnight, washed with TBST three times, incubated with HRP-conjugated secondary antibodies for 1h at room temperature and detected using a Westar Supernova kit (Cyanagen).

Statistical analysis

GraphPad Prism 5 was used for statistical analysis. In histograms, all data are presented as the mean ± SD of at least three independent replicates for each experiment. The statistical significance of the data was assessed by Student's two-tailed unpaired t-test or two-way ANOVA (*$p < 0.05$; **$p < 0.01$; ***$p < 0.001$).

Results

H_2O_2 enhances the anticancer activity of TMPyP4 on A549 and PANC cells but has no superimposed cytotoxicity on normal hepatic MIHA cells

First, we examined whether H_2O_2 enhanced the antitumor effect of TMPyP4, and the cell viability assay suggested that H_2O_2 significantly increased the cell viability inhibitory effect of TMPyP4 on A549 and PANC cells within the concentration range of 0-50 μM but had no effect on normal hepatic MIHA cells (Supplementary Figure 1). In addition, it has been verified that the concentration of H_2O_2 in the TME could be as high as millimolar levels [23, 24]. Therefore, the best concentrations of TMPyP4 (10 μM) and H_2O_2 (800 μM) were chosen for the following experiments.

The results showed that compared to TMPyP4 treatment alone, the combination of TMPyP4 and H_2O_2 had a stronger cell viability inhibitory effect on A549 and PANC cells without superimposed cytotoxicity on MIHA cells (Figure 1A-1C). Moreover, the colony formation assay indicated that H_2O_2 strengthened the inhibitory effect of TMPyP4 on A549 and PANC cell colony formation ability (Figure 1D and 1E). Furthermore, the apoptosis assay indicated that H_2O_2 selectively increased the number of TMPyP4-induced apoptotic A549 and PANC cells but not MIHA cells (Figure 1F and 1G). Taken together, these results revealed that H_2O_2 enhanced the anticancer activity of TMPyP4 on A549 and PANC cells by inhibiting cell viability, suppressing colony formation and enhancing cell apoptosis.

H_2O_2 increases TMPyP4-induced ROS production in A549 and PANC cells

It is well known that as a photosensitizer, TMPyP4 produces a large amount of ROS, and high levels of ROS can cause oxidative distress to cells, leading to damage to biomolecules and apoptosis [25]. Therefore, it is reasonable to assume that TMPyP4 combined with H_2O_2 might generate more ROS than TMPyP4 alone in A549 and PANC cells. The FACS results showed that H_2O_2 could potentiate ROS production in TMPyP4-treated A549 and PANC cell lines (Figure 2A-2D). These results were consistent with the data from fluorescence assays, which showed that TMPyP4 combined with H_2O_2-treated cells had higher intracellular ROS levels than TMPyP4- or H_2O_2-treated cells alone (Figure 2E). Collectively, these data indicate that H_2O_2 enhances the anticancer activity of TMPyP4 by raising intracellular ROS levels in A549 and PANC cells.

H_2O_2 enhances TMPyP4-induced apoptosis through a mitochondria-mediated pathway

It is generally thought that increased ROS levels are due to a perturbed intracellular redox status, which induces mitochondrial dysfunction [26]. Loss of mitochondrial membrane potential (Δψm) is detrimental to cells and leads to the release of cytochrome C into the cytosol [27]. We detected the mitochondrial membrane potential through FACS flow cytometry by using the JC-1 dye. The data revealed that compared to TMPyP4 alone, the combination of TMPyP4 and H_2O_2 significantly decreased the mitochondrial membrane potential in both A549 and PANC cells (Figure 3A-3C). Next, the expression of the mitochondrial-mediated apoptosis pathway-associated proteins Bax and Bcl-2 was measured by western blot assay. Compared to TMPyP4 or H_2O_2 treatment alone, TMPyP4 combined with H_2O_2 treatment markedly increased the ratio of Bax/Bcl-2 in A549 and PANC cells (Figure 3D and 3E). In addition, the results of fluorescent staining and western blot analysis demonstrated that compared to TMPyP4 or H_2O_2 treatment alone, TMPyP4 combined with H_2O_2 treatment increased the expression of cleaved caspase 3 in A549 and PANC cells (Figure 3F-3H). It has been well established that

mitochondrial-dependent cell apoptosis involves alteration of the BAX/Bcl-2 proteins by c-Jun N-terminal kinase (JNK) [28-30]. Our results revealed that TMPyP4 combined with H_2O_2 treatment dramatically increased the expression of p-JNK compared to the single-agent treatment in A549 and PANC cells (Figure 3I). Taken together, the present results showed that H_2O_2 enhances TMPyP4-induced apoptosis through a mitochondria-mediated pathway.

H_2O_2 aggravates TMPyP4-induced DNA damage and the DNA damage response in A549 and PANC cells.

Increased and accumulated ROS have previously been reported to cause oxidative DNA damage, including single-stranded breaks, double-stranded breaks and others [31, 32]. The alkaline comet assay and neutral comet assay that can detect multiple DNA lesions (SSBs, DSBs, and alkali-labile sites) were first performed to measure the DNA lesions in A549 and PANC cells treated with TMPyP4, H_2O_2 or TMPyP4 combined with H_2O_2. As expected, the results show that compared to single agent treatment, the combination of TMPyP4 and H_2O_2 caused more intense DNA damage in A549 and PANC (Figure 4A-4D and Supplementary Figure 2) cells. Moreover, the IF assay indicated that compared to TMPyP4 or H_2O_2 treatment alone, TMPyP4 combined with H_2O_2 treatment provoked more 53BP1 foci per cell in the A549 (Figure 4E and 4G) and PANC cells (Figure 4F and 4H), revealing intense accumulation of DSBs in these cells, provoking strong DNA damage response. These results were consistent with western blot analysis data, which demonstrated that significantly increased expression of γ-H2AX was observed in A549 and PANC cells in the TMPyP4 and H_2O_2 co-treatment group compared with the TMPyP4 or H_2O_2 treatment alone (Figure 4I and 4J). Collectively, these data suggested that H_2O_2 potentiates TMPyP4-induced DNA damage and the DNA damage response in A549 and PANC cell lines.

Discussion

TMPyP4 has already attracted a substantial amount of attention due to its dual role in PDT and telomerase treatment [14, 18, 19]. However, most cells used in TMPyP4-related studies were cultured in a traditional culture environment with no or diminished ROS levels. The tumor microenvironment (TME) is known to have a high ROS level [1]. Consequently, it is difficult to achieve equivalent *in vivo* application values based on the results from cells *in vitro*. The present study provides evidence that H_2O_2 enhanced the anticancer activity of TMPyP4, including promoting TMPyP4-induced reductions in cell viability and colony formation, as well as cell apoptosis (Fig. 1). The underlying mechanism behind the synergistic anticancer effects of TMPyP4 and H_2O_2 on A549 and PANC cells is summarized in Fig. 5. This finding is of interest because high intracellular ROS levels are a typical characteristic of the TME.

It has been found that unbalanced intracellular ROS levels are harmful to cells, resulting in intense DNA damage leading to cell apoptosis [33, 1]. Because of this, ROS have been considered a valuable therapeutic target in the TME. Our results showed that the intracellular ROS levels increased significantly

in TMPyP4 combined with H_2O_2-treated A549 and PANC cells compared to TMPyP4- or H_2O_2-treated alone groups when using a sensitive free-radical indicator DCFH-DA probe (Fig. 2). Since intracellular ROS are mainly produced by mitochondria [7], it has been proposed that H_2O_2 enhances the anticancer activity of TMPyP4 *via* a ROS-mediated mitochondria-dependent pathway. The elevation of JC-1 green fluorescence indicated the loss of mitochondrial membrane potential in TMPyP4 combined H_2O_2 treated A549 cells and PANC cells compared to TMPyP4 or H_2O_2 treated alone groups (Fig. 3A-3C). Mitochondrial function disruption affects the regulation and expression of apoptosis-related proteins [34, 35]. Hence, the data in the present study suggested that TMPyP4 combined with H_2O_2 treatment upregulated the expression of pro-apoptotic protein Bax and downregulated the anti-apoptotic protein Bcl-2 (Fig. 3D), leading to an increased ratio of Bax/Bcl2 in TMPyP4 combined H_2O_2-treated A549 cells and PANC cells (Fig. 3E). Furthermore, increased activity of cleaved caspase 3 and phosphorylated JNK (p-JNK) in TMPyP4 and H_2O_2-treated A549 cells and PANC cells (Fig. 3F-3I) further indicated that apoptosis enhanced by H_2O_2 is a ROS-mediated mitochondria-dependent pathway [34, 36].

Unbalanced intracellular ROS trigger strong DNA damage and DNA damage responses [32]. Our results showed that H_2O_2 enhanced TMPyP4-induced DNA damage and provoked stronger DNA damage response. Taken together, the data in the present study suggested that H_2O_2 enhanced the anticancer activity of TMPyP4 by disrupting ROS-mediated mitochondrial function, upregulating apoptosis-related proteins, triggered intense DNA damage and provoking a strong DNA damage response. This effect was not observed in normal human hepatocyte MIHA cells, indicating the advantages of TMPyP4 in cancer treatment.

In conclusion, these data suggested that H_2O_2 enhanced the anticancer activity of TMPyP4-mediated ROS-dependent mitochondrial dysfunction, leading to upregulation of apoptosis-related protein expression and triggering DNA damage. These findings contribute to a better understanding of the biological effects induced by TMPyP4 and provide new insight into the effects of a high ROS tumor microenvironment.

Declarations

Funding

The present study was funded by National Science Foundation of China (No. 21701194), Wenzhou Basic Medical and Health Technology Project (Y20180177) and Wenzhou Medical University Talent Start-up Fund (QTJ17022) for the financial support.

Conflicts of interest

The authors report no declarations of interest.

Availability of data and material

The data real reliable.

Code availability

Not applicable.

Authors' contributions

Conceptualization: XHZ, GL, XDZ, JQC. Methodology and Data analysis：JQC, XXJ, ZS, YM, JFZ. Writing - original draft preparation: XZ, JC. Funding acquisition and supervision: XHZ, GL, XDZ.

Ethics approval

Not applicable.

Consent to participate

All authors have approved this work.

Consent for publication

All authors agree to publish.

Acknowledgements

We thank Elsevier (http://webshop.elsevier.com/languageediting/) for its linguistic assistance during the preparation of this manuscript.

References

1. Weinberg F, Ramnath N, Nagrath D. Reactive Oxygen Species in the Tumor Microenvironment: An Overview. Cancers (Basel). 2019;11(8). doi:10.3390/cancers11081191.
2. Szatrowski TP, Nathan CF. Production of large amounts of hydrogen peroxide by human tumor cells. Cancer Res. 1991;51(3):794-8.
3. Lopez-Lazaro M. Dual role of hydrogen peroxide in cancer: possible relevance to cancer chemoprevention and therapy. Cancer Lett. 2007;252(1):1-8. doi:10.1016/j.canlet.2006.10.029.

4. Buettner GR, Ng CF, Wang M, Rodgers VG, Schafer FQ. A new paradigm: manganese superoxide dismutase influences the production of H2O2 in cells and thereby their biological state. Free Radic Biol Med. 2006;41(8):1338-50. doi:10.1016/j.freeradbiomed.2006.07.015.
5. Weinberg F, Hamanaka R, Wheaton WW, Weinberg S, Joseph J, Lopez M et al. Mitochondrial metabolism and ROS generation are essential for Kras-mediated tumorigenicity. Proc Natl Acad Sci U S A. 2010;107(19):8788-93. doi:10.1073/pnas.1003428107.
6. Weinberg F, Chandel NS. Reactive oxygen species-dependent signaling regulates cancer. Cell Mol Life Sci. 2009;66(23):3663-73. doi:10.1007/s00018-009-0099-y.
7. Okon IS, Coughlan KA, Zhang M, Wang Q, Zou MH. Gefitinib-mediated reactive oxygen specie (ROS) instigates mitochondrial dysfunction and drug resistance in lung cancer cells. J Biol Chem. 2015;290(14):9101-10. doi:10.1074/jbc.M114.631580.
8. Dharmaraja AT. Role of Reactive Oxygen Species (ROS) in Therapeutics and Drug Resistance in Cancer and Bacteria. J Med Chem. 2017;60(8):3221-40. doi:10.1021/acs.jmedchem.6b01243.
9. Cui Q, Wang JQ, Assaraf YG, Ren L, Gupta P, Wei L et al. Modulating ROS to overcome multidrug resistance in cancer. Drug Resist Updat. 2018;41:1-25. doi:10.1016/j.drup.2018.11.001.
10. Yang H, Villani RM, Wang H, Simpson MJ, Roberts MS, Tang M et al. The role of cellular reactive oxygen species in cancer chemotherapy. J Exp Clin Cancer Res. 2018;37(1):266. doi:10.1186/s13046-018-0909-x.
11. Pervaiz S, Olivo M. Art and science of photodynamic therapy. Clin Exp Pharmacol Physiol. 2006;33(5-6):551-6. doi:10.1111/j.1440-1681.2006.04406.x.
12. Benov L. Photodynamic therapy: current status and future directions. Med Princ Pract. 2015;24 Suppl 1:14-28. doi:10.1159/000362416.
13. Debele TA, Peng S, Tsai HC. Drug Carrier for Photodynamic Cancer Therapy. Int J Mol Sci. 2015;16(9):22094-136. doi:10.3390/ijms160922094.
14. Pushpan SK, Venkatraman S, Anand VG, Sankar J, Parmeswaran D, Ganesan S et al. Porphyrins in photodynamic therapy - a search for ideal photosensitizers. Curr Med Chem Anticancer Agents. 2002;2(2):187-207. doi:10.2174/1568011023354137.
15. Villanueva A, Caggiari L, Jori G, Milanesi C. Morphological aspects of an experimental tumour photosensitized with a meso-substituted cationic porphyrin. J Photochem Photobiol B. 1994;23(1):49-56. doi:10.1016/1011-1344(93)06982-9.
16. Awan MA, Tarin SA. Review of photodynamic therapy. Surgeon. 2006;4(4):231-6. doi:10.1016/s1479-666x(06)80065-x.
17. Tada-Oikawa S, Oikawa S, Hirayama J, Hirakawa K, Kawanishi S. DNA damage and apoptosis induced by photosensitization of 5,10,15,20-tetrakis (N-methyl-4-pyridyl)-21H,23H-porphyrin via singlet oxygen generation. Photochem Photobiol. 2009;85(6):1391-9. doi:10.1111/j.1751-1097.2009.00600.x.
18. Konieczna N, Romaniuk-Drapala A, Lisiak N, Toton E, Paszel-Jaworska A, Kaczmarek M et al. Telomerase Inhibitor TMPyP4 Alters Adhesion and Migration of Breast-Cancer Cells MCF7 and MDA-

MB-231. Int J Mol Sci. 2019;20(11). doi:10.3390/ijms20112670.

19. Zheng XH, Nie X, Liu HY, Fang YM, Zhao Y, Xia LX. TMPyP4 promotes cancer cell migration at low doses, but induces cell death at high doses. Sci Rep. 2016;6:26592. doi:10.1038/srep26592.
20. Mikami-Terao Y, Akiyama M, Yuza Y, Yanagisawa T, Yamada O, Yamada H. Antitumor activity of G-quadruplex-interactive agent TMPyP4 in K562 leukemic cells. Cancer Lett. 2008;261(2):226-34. doi:10.1016/j.canlet.2007.11.017.
21. Zheng XH, Nie X, Fang YM, Zhang ZP, Xiao YN, Mao ZW et al. A Cisplatin Derivative Tetra-Pt(bpy) as an Oncotherapeutic Agent for Targeting ALT Cancer. Jnci-J Natl Cancer I. 2017;109(10). doi:ARTN djx061 10.1093/jnci/djx061.
22. Olive PL, Banath JP. The comet assay: a method to measure DNA damage in individual cells. Nat Protoc. 2006;1(1):23-9. doi:10.1038/nprot.2006.5.
23. Park WH. MAPK inhibitors, particularly the JNK inhibitor, increase cell death effects in H2O2-treated lung cancer cells via increased superoxide anion and glutathione depletion. Oncol Rep. 2018;39(2):860-70. doi:10.3892/or.2017.6107.
24. Rhee SG, Kang SW, Jeong W, Chang TS, Yang KS, Woo HA. Intracellular messenger function of hydrogen peroxide and its regulation by peroxiredoxins. Curr Opin Cell Biol. 2005;17(2):183-9. doi:10.1016/j.ceb.2005.02.004.
25. Sies H. Hydrogen peroxide as a central redox signaling molecule in physiological oxidative stress: Oxidative eustress. Redox Biol. 2017;11:613-9. doi:10.1016/j.redox.2016.12.035.
26. Wang WJ, Mao LF, Lai HL, Wang YW, Jiang ZB, Li W et al. Dolutegravir derivative inhibits proliferation and induces apoptosis of non-small cell lung cancer cells via calcium signaling pathway. Pharmacol Res. 2020;161:105129. doi:10.1016/j.phrs.2020.105129.
27. Weinberg SE, Chandel NS. Targeting mitochondria metabolism for cancer therapy. Nat Chem Biol. 2015;11(1):9-15. doi:10.1038/nchembio.1712.
28. Lei K, Davis RJ. JNK phosphorylation of Bim-related members of the Bcl2 family induces Bax-dependent apoptosis. Proc Natl Acad Sci U S A. 2003;100(5):2432-7. doi:10.1073/pnas.0438011100.
29. Ma L, Wei J, Wan J, Wang W, Wang L, Yuan Y et al. Low glucose and metformin-induced apoptosis of human ovarian cancer cells is connected to ASK1 via mitochondrial and endoplasmic reticulum stress-associated pathways. Journal of Experimental & Clinical Cancer Research. 2019;38(1). doi:10.1186/s13046-019-1090-6.
30. Chen X, Zhao Y, Luo W, Chen SA, Lin F, Zhang X et al. Celastrol induces ROS-mediated apoptosis via directly targeting peroxiredoxin-2 in gastric cancer cells. Theranostics. 2020;10(22):10290-308. doi:10.7150/thno.46728.
31. Trachootham D, Alexandre J, Huang P. Targeting cancer cells by ROS-mediated mechanisms: a radical therapeutic approach? Nat Rev Drug Discov. 2009;8(7):579-91. doi:10.1038/nrd2803.
32. Srinivas US, Tan BWQ, Vellayappan BA, Jeyasekharan AD. ROS and the DNA damage response in cancer. Redox Biol. 2019;25:101084. doi:10.1016/j.redox.2018.101084.

33. Sies H. Role of reactive oxygen species in biological processes. Klin Wochenschr. 1991;69(21-23):965-8. doi:10.1007/BF01645140.
34. Ly JD, Grubb DR, Lawen A. The mitochondrial membrane potential (deltapsi(m)) in apoptosis; an update. Apoptosis. 2003;8(2):115-28. doi:10.1023/a:1022945107762.
35. Shim HY, Park JH, Paik HD, Nah SY, Kim DS, Han YS. Acacetin-induced apoptosis of human breast cancer MCF-7 cells involves caspase cascade, mitochondria-mediated death signaling and SAPK/JNK1/2-c-Jun activation. Mol Cells. 2007;24(1):95-104.
36. Liu J, Lin A. Role of JNK activation in apoptosis: a double-edged sword. Cell Res. 2005;15(1):36-42. doi:10.1038/sj.cr.7290262.

Figures

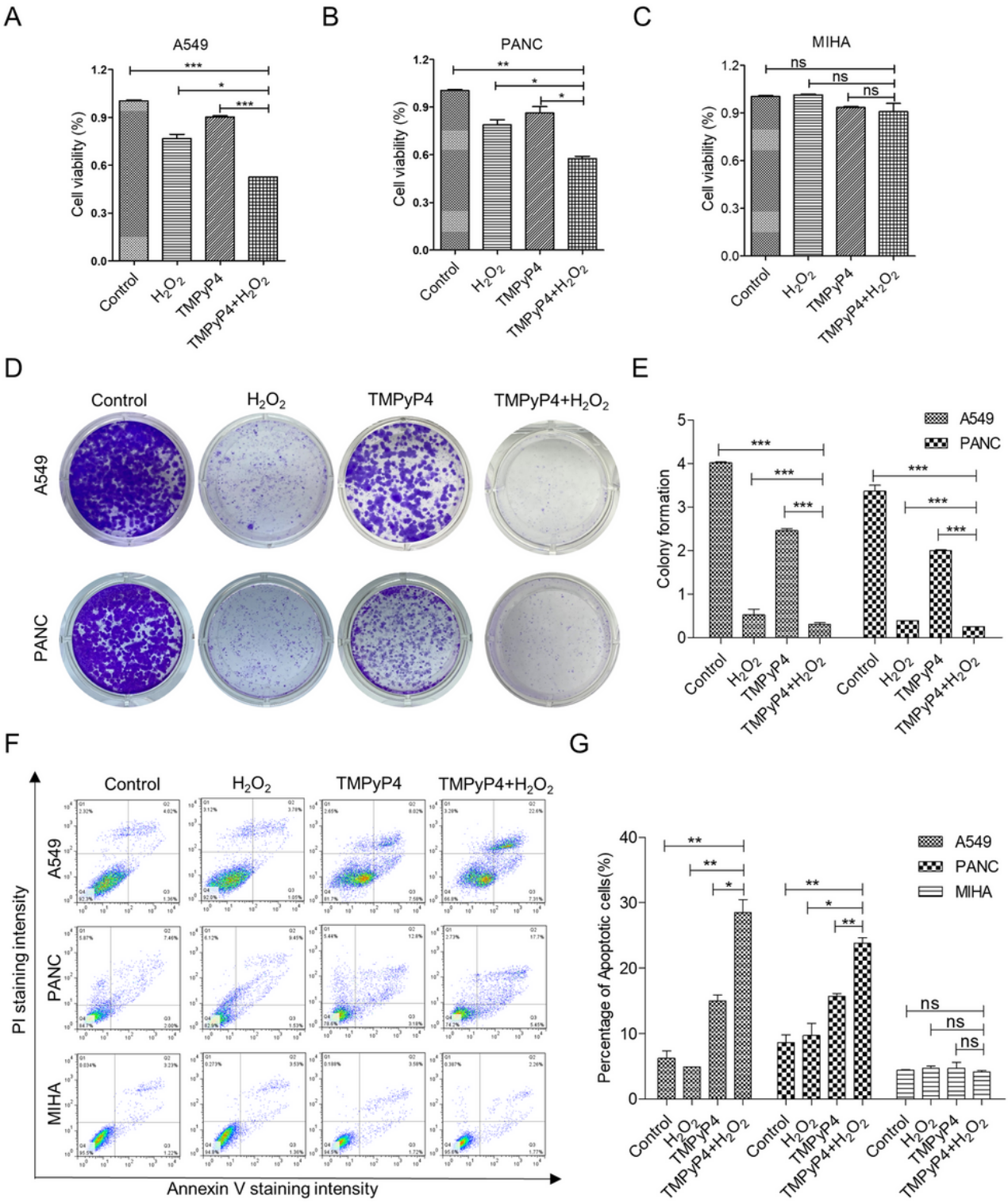

Figure 1

H2O2 enhances the antitumor activity of TMPyP4 in A549 and PANC cell lines but has no superimposed cytotoxicity on normal hepatic MIHA cells. (A, B and C) A549, PANC and MIHA cells were exposed to TMPyP4 (10 μM) for 70 h and then incubated with 800 μM H2O2 for another 2 hours. Cell viability was detected by MTT assays. (D) Colony formation analysis for cell proliferation evaluation. (E) Quantification of D. (F) H2O2 enhanced TMPyP4-induced apoptosis in A549 and PANC cells as measured

by Annexin V/PI staining but did not increase apoptosis in normal hepatic MIHA cells. (G) Quantification of F. Values represent the mean ± standard deviation (SD) of at least three independent experiments. Statistical significance was calculated using unpaired Student's two-tailed t-tests (*p<0.05, **p<0.01, ***p<0.001).

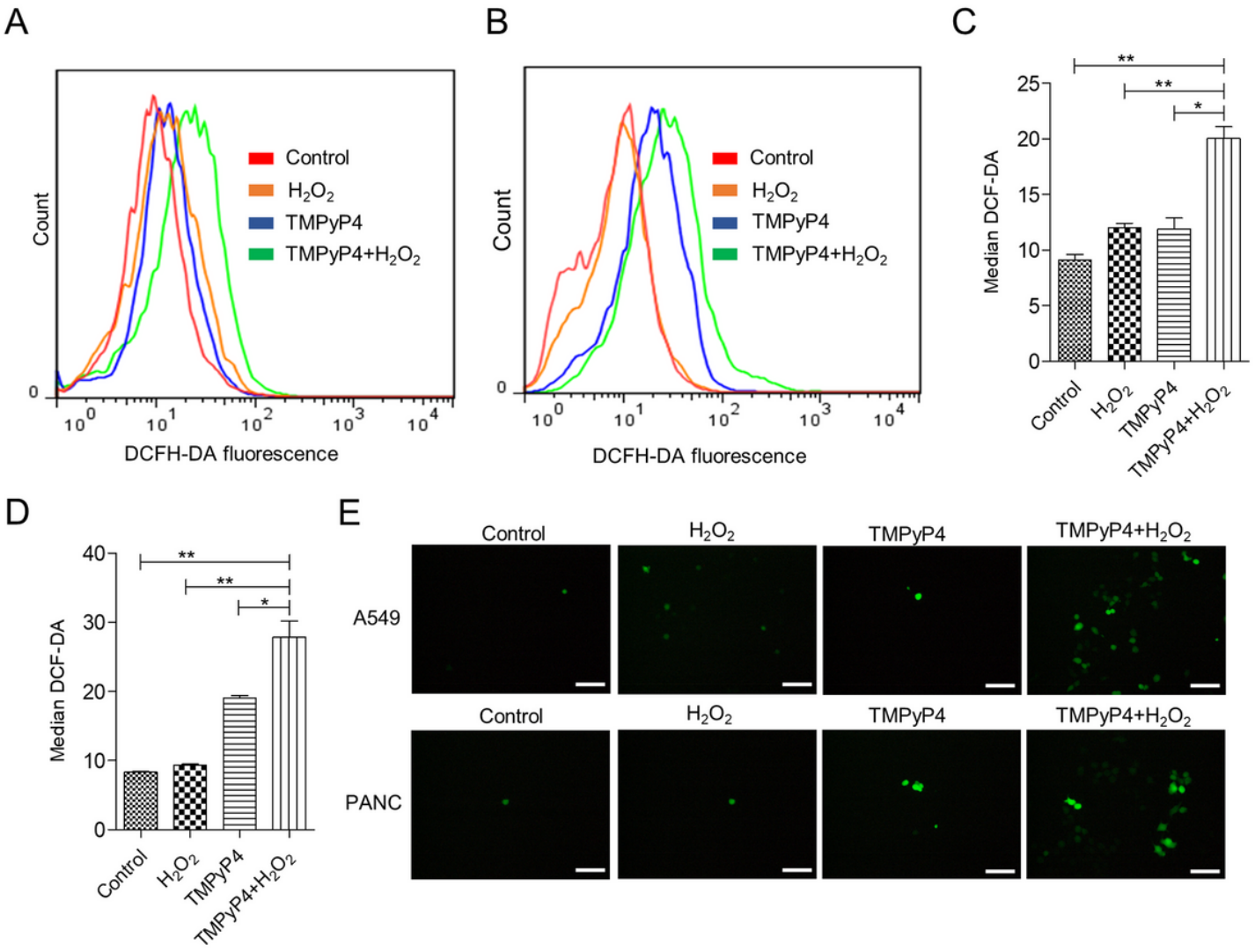

Figure 2

H2O2 potentiates TMPyP4-induced ROS generation in A549 and PANC cell lines. A549 (A) and PANC (B) cells were treated with 10 μM TMPyP4 for 70 hours, and then 800 μM H2O2 was added for another 2 hours. Then, all cells were collected for DCFH-DA staining and measured by FACS. Data analysis was carried out with FlowJo 7.1. (C) Quantification of ROS levels in A549 cells. (D) The same as C, except PANC cells were used. (E) Representative DCF fluorescence intensity images of the cells. Scale bar, 100 μm. The values are presented as the mean ± SD of at least three independent experiments. Statistical significance was calculated using unpaired Student's two-tailed t tests (*p<0.05, **p<0.01, ***p<0.001).

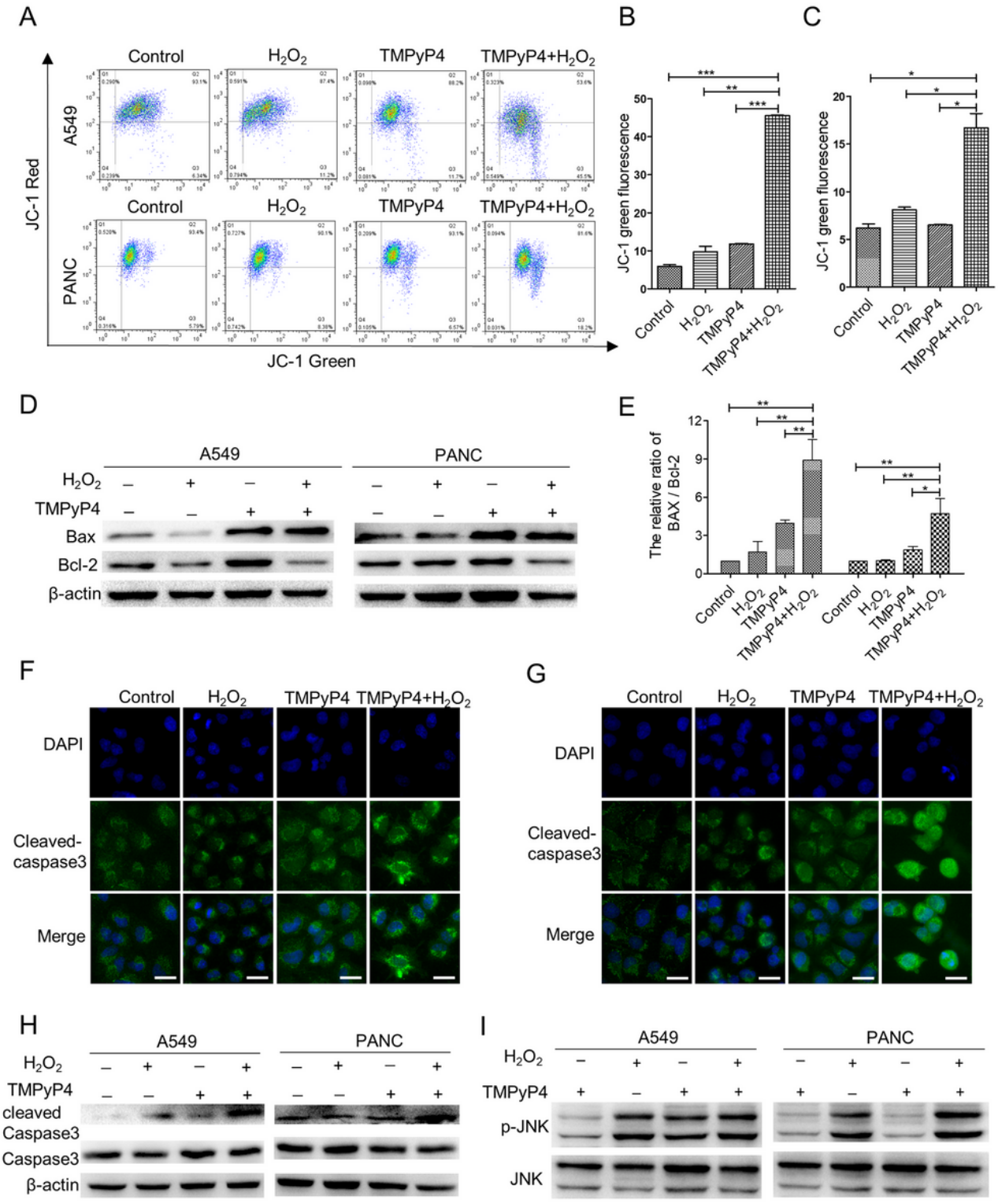

Figure 3

H2O2 enhances TMPyP4-induced apoptosis through a mitochondrial-associated apoptosis pathway in A549 and PANC cells. (A) Mitochondrial membrane potential (Δψm) was measured by flow cytometry using JC-1 staining. Cells were incubated with TMPyP4 (10 μM) for 70 hours, and then H2O2 (800 μM) was added for another 2 hours. (B and C) Quantification of A. (D) Western blot analysis of the expression of Bax and Bcl-2 proteins in cells treated with TMPyP4 (10 μM) for 70 hours, and then H2O2 (800 μM)

was added for another 2 hours. (E) Quantification of D. (F) The expression of cleaved caspase 3 in A549 cells was examined by fluorescence microscopy. Scale bar, 50 μm. (G) The same as F, except PANC cells were used. (H) Western blot analysis of caspase 3 and cleaved caspase 3. (I) Western blot analysis of JNK phosphorylation. JNK protein was used as the internal control. Values are presented as the mean ± SD of at least three independent experiments. Statistical significance was calculated using unpaired Student's two-tailed t-tests (*p<0.05, **p<0.01, ***p<0.001).

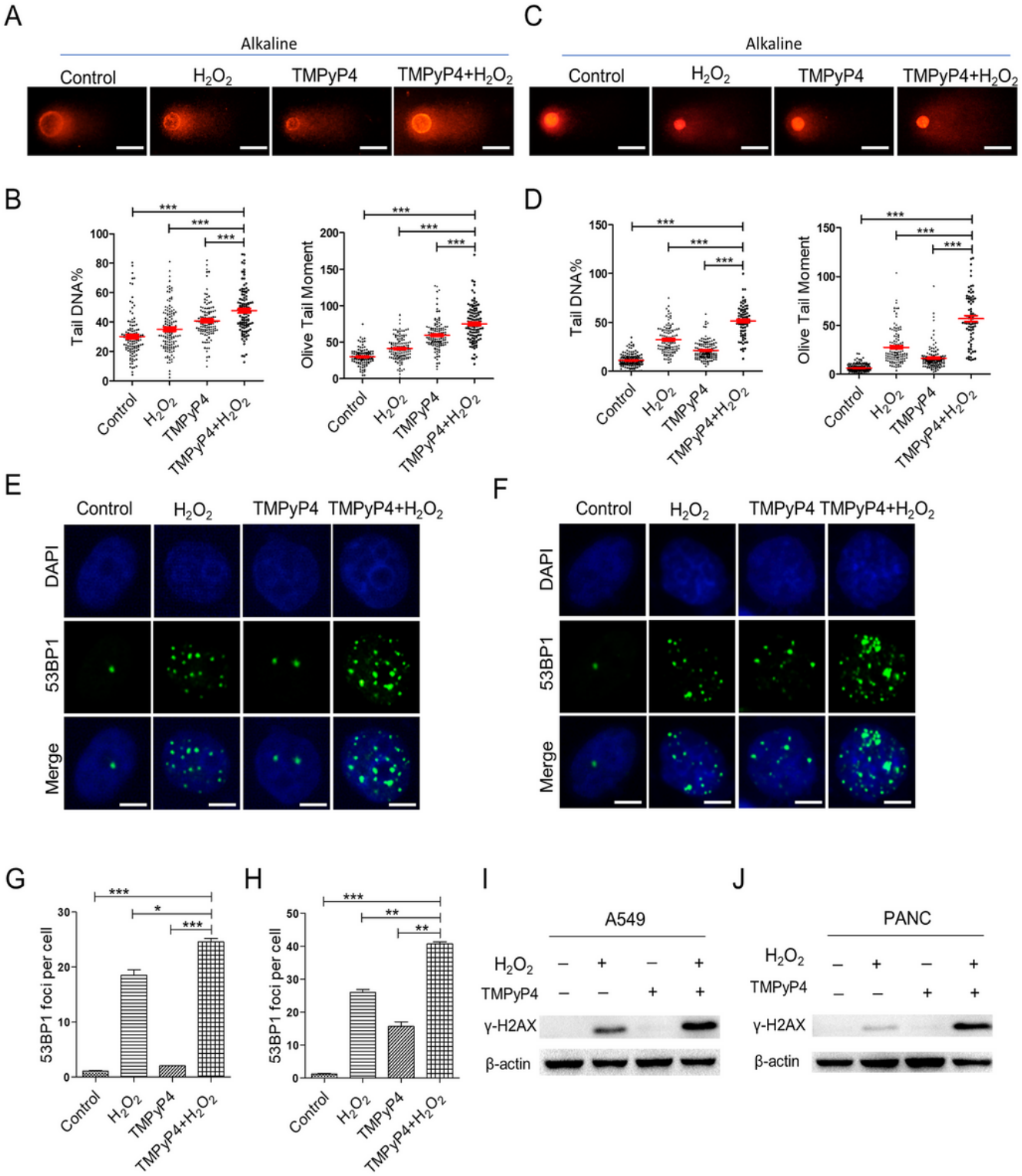

Figure 4

H2O2 enhanced TMPyP4-induced DNA damage in A549 and PANC cell lines. (A, C) The alkaline comet assay was performed to detect DNA damage in A549 (A) and PANC (C) cells exposed to TMPyP4 (10 μM) for 70 hours and then incubated with H2O2 (800 μM) for another 2 hours. Scale bar, 100 μm. (B, D) Quantification of A and C, respectively. Statistics of tail DNA% and olive tail moment reflect the degree of DNA damage, and ≥200 cells were examined in each group. (E, F) The accumulation of 53BPl nuclear foci as a marker of the DNA damage response was investigated by IF in A549 and PANC cells. Scale bar, 10 μm. (G) and (H) Quantification of E and F, respectively. More than 200 cells were counted in each group. (I, J) Western blot analysis of γ-H2AX. Values are presented as the mean ± SD of at least three independent experiments. Statistical significance was calculated using unpaired Student's two-tailed t-tests (*p<0.05, **p<0.01, ***p<0.001).

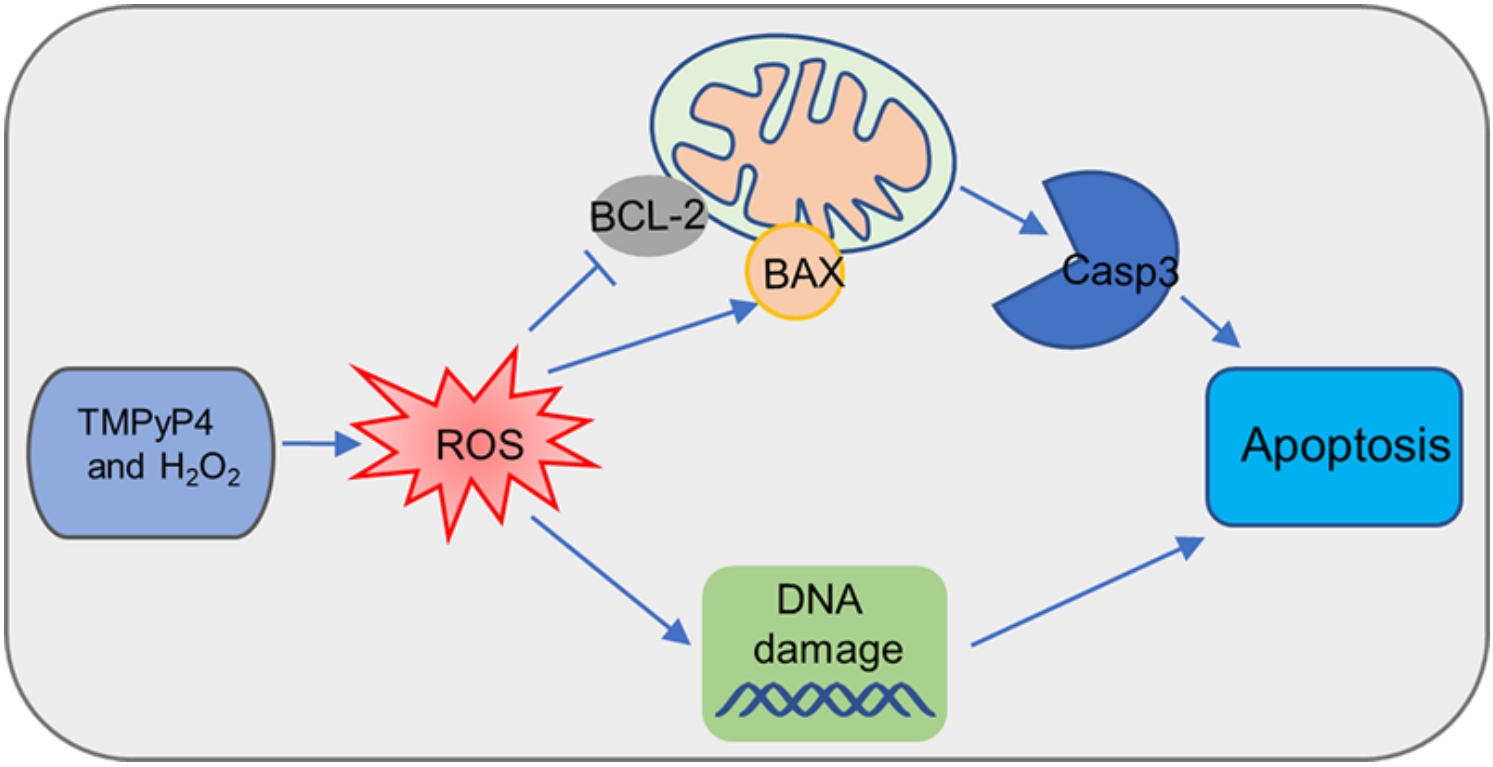

Figure 5

Schematic illustration of key findings of the present study. H2O2 elevated TMPyP4-induced ROS, then decreased mitochondrial membrane potential, up-regulated the expression of mitochondrial-mediated apoptosis pathway associated protein and triggered DNA damage which were contributed to cell apoptosis.

Supplementary Files

This is a list of supplementary files associated with this preprint. Click to download.

- Supplementarymaterial.docx
- Originalimagesforallblotsinourfigures.docx